Journal of Engineering and Applied Sciences 12 (Special Issue 7): 8217-8223, 2017
ISSN: 1816-949X

Independent Control of Hybrid Bearingless Switched Reluctance Motor using Single Neuron Sliding Mode Controller

[1]Polamraju V.S. Sobhan, [2]G.V. Nagesh Kumar and [3]P.V. Ramana Rao
[1]Department of EEE, VFSTR University, Guntur, India
[2]Department of EEE, Vignan's Institute of Information, Technology, Visakhapatnam, India
[3]Department of EEE, Acharya Nagarjuna University, Guntur, India

Abstract: This study deals with the control of a 12/14 hybrid pole type bearingless switched reluctance motor which is a highly non-linear, multi variable and open loop unstable system. A novel control method for suspending the rotor and regulating the speed of the BSRM based on decoupled nature of torque and suspension force is discussed. The proposed control strategy integrates a neuron with auto-tuning and the sliding mode control in order to eliminate the rotor eccentricity error and torque ripples. Experimental results demonstrate that the proposed auto tuning neuron-sliding mode controller guarantees stable suspension as well as the speed tracking.

Key words: BSRM, suspending force control, auto tuning neuron-sliding mode controller, rotor eccentricity, stable, motor

INTRODUCTION

The mechanical bearings in motors create many problems such as mechanical wearing, thermal problem, increase of frictional drag and decrease in operational life of bearings. Also, the use of lubricants makes the motor difficult to operate in high purity environments such as space, semiconductor, pharmaceutical and radioactive (Bosch, 1988; Bichsel, 1991; Ooshima and Takeuchi, 2011). The shortcomings of mechanical bearings can be addressed by opting for magnetic-bearing motors. The bearingless motor is an electrical combination of motor and magnetic bearing. Besides, torque control this motor necessitates non contact rotor levitation (Fukao, 2000; Okada *et al*., 2005; Shen *et al*., 2000). Bearingless motors have many advantages such as compact size, lubrication and seal free performance, long life, low cost, high speed and high power (Hertel and Hofmann, 2000). The switched reluctance motor is a natural choice as a bearingless motor owing to its magnetic attraction between stator poles and rotor poles which produces the torque to drive the rotor. In addition the rotor experiences a high amount of radial force which can be used effectively for suspending the rotor shaft (Lee and Ahn, 2011).

The majority of the proposed Bearingless Switched Reluctance Motor (BSRM) structures are based on conventional SRM structure which complicates the rotor eccentricity control due to the existence of coupling between the suspending force and the torque control. Takemoto *et al*. (2002) proposed differentially wounded BSRMs in which an auxiliary suspending winding and torque winding are wound on each stator pole and are controlled by different power converters (Takemoto *et al*., 2000). In the single winding structure proposed by Chen three torques and three suspending forces are produced due to energization of windings by currents in each commutating period. The produced torque and suspending force are the summation of the three torques and suspending strengths of each winding (Chen and Hofmann, 2006; 2007). In the hybrid rotor structure proposed by Morrison *et al*., the rotor is made up of two laminated segments, circular segment used for suspension and multipole segment used for both suspension and torque generation (Wang *et al*., 2011). In all the aforesaid designs, as the control of suspending force is coupled with torque they cannot guarantee the full utilization of generating torque and radial force regions and selection of operating point is a compromise between the two forces. Wang *et al*. (2011) proposed hybrid BSRM by separating suspending force pole with torque pole to minimize the interdependency of two forces. Due to this decoupling poles, the suspending force control can be achieved easily.

Corresponding Author: Polamraju V.S. Sobhan, Department of EEE, VFSTR University, Guntur, India

The suspension control of the hybrid BSRM rotor is quite a challenging problem due to its inherently high nonlinearity and uncertainty. Zhenyao Xu *et al.* proposed one PI controller for speed control and two independent PID controllers for controlling the rotor radial displacement in both directions (x and y). The tuning of PID controller parameters is a time consuming process and poor tuning results in rotor eccentricity, torque pulsations and hence, speed ripples due to high nonlinear variation of each phase inductance.

In this study, a sliding mode controller which integrates with an auto-tuning single neuron is proposed for rotor suspension and torque control of BSRM drive by considering load disturbances. Elimination of chattering when the state trajectory enters into the boundary layer can be achieved by activating the direct adaptive single neuron instead of the sliding mode control. Two independent, non-model-based SNSM controllers for suspension force control and the torque control by avoiding the modeling complexity are proposed. Experimental results demonstrate that the proposed controller keeps rotor eccentricity and speed error within a narrow band near zero and minimizing torque ripples.

Hybrid pole type BSRM, structure and operation

BSRM structure: The basic structure of 12/14 hybrid pole type BSRM is shown in Fig. 1. The 12 stator poles are wound with two different windings, 8 poles for torque production and 4 poles for suspension force. This arrangement helps to decouple suspension force from the torque. Since, the suspension force pole arc is made slightly more than one rotor pole pitch, the available overlap area between suspension force pole and rotor pole become constant, compared with conventional bearingless SRM. This design completely decouples the suspending force control from torque control due to negligible undesirable torque produced by suspending force poles. The rotational torque is produced by A and B phases which are formed by connecting 4 torque pole windings P_{A1}-P_{A4} in series and other 4 torque pole windings P_{B1}-P_{B4} in series, respectively. The torque control can be achieved by controlling two phase currents i_A and i_B. The x and y-directional suspension forces are generated by the suspending winding currents i_{xp} and i_{xn}, i_{yp} and i_{yn} flowing in the poles P_{xp} and P_{xn}, P_{yp} and P_{yn}, respectively. The suspending force on the rotor in both positive and negative x and y directions can be controlled by controlling i_{xp}, i_{xn}, i_{yp} and i_{yn} independently.

Torque control: The electromagnetic torque produced by torque poles P_A and P_B is given in Eq. 1 and the torque profile mainly depends on the inductance profile:

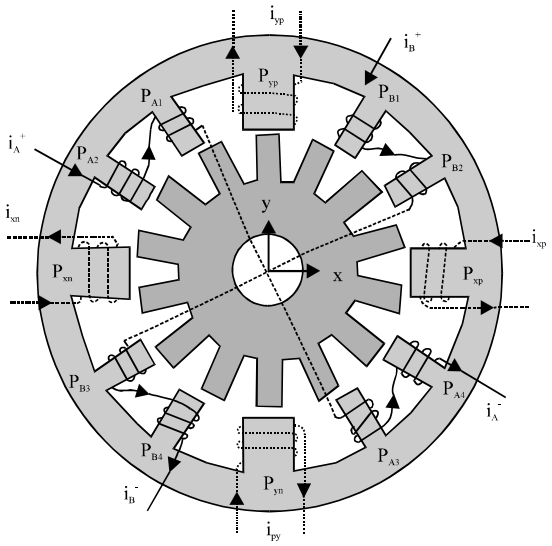

Fig. 1: Suspension and torque winding structure of 12/14 BSRM

$$T = \frac{1}{2} i^2 \frac{dL}{d\theta} \quad (1)$$

In the hybrid BSRM, the suspension winding inductance profile is almost constant with the constant suspending current and hence the variation of inductance with reference to rotor position is negligible and the torque is independent of suspending force current. In the case of torque winding, the inductance variation with reference to rotor position is considerably large due to large variation in the inductance profile from aligned to unaligned position and hence the total torque on the rotor is due to torque winding only.

Suspending force control: The absence of mechanical bearings in BSRM causes displacement of the rotor from the center position leading to eccentricity. Figure 2 shows the rotor eccentricity due to unbalanced pull force directed in the fourth quadrant of x-y plane and the required compensating suspending force F on the rotor which is in the direction of second quadrant. The rotor movement towards the central position is controlled by the controller using the signals from the power amplifier and the four displacement sensors which detects the rotor eccentricity. The net suspending force F is a resultant of F_x and F_y where F_x is the generated radial force in the negative x-direction due to i_{xp} in pole P_{xn} and F_y is the generated radial force in the positive y-direction due to i_{yp} in pole P_{yp}. The magnitude of F in any desired direction can be controlled by regulating the four suspending force winding currents i_{xp}, i_{xn}, i_{yp} and i_{yn}.

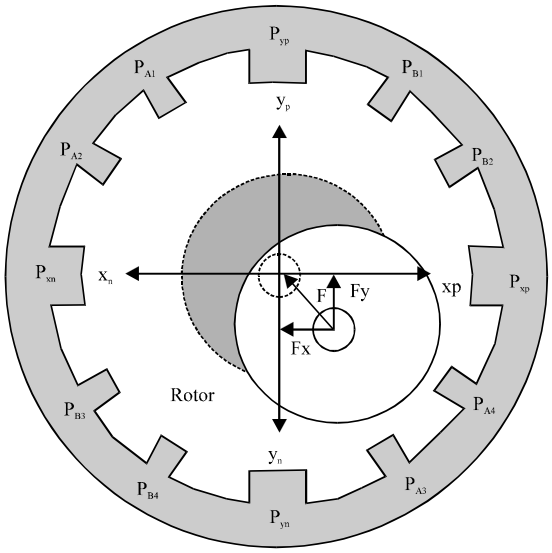

Fig. 2: Radial displacement of rotor and suspension force

MATERIALS AND METHODS

Single neuron-sliding mode control: To control the rotor suspension and speed, the conventional PID controller is less preferable due to time consuming tuning methods and constant values of tuned proportional, integral and differential gains (K_p, K_i, K_d) are largely affected by variations in system parameters, load and speed. So, the alternative control scheme is the combined auto tuning neuron with Variable Structure Control (VSC) to obtain high-performance control for the BSRM system.

Sliding Mode Control (SMC): The SMC is a class of variable structure control of linear and nonlinear systems with features such as rapid dynamic response, robust and insensitive to parameter variations and disturbances. An nth-order uncertain non-linear system is represented as:

$$\begin{aligned} \dot{x}_i &= x_{i+1}\,(i = 1, 2, \ldots, n\text{-}1) \\ \dot{x}_n &= f(x_1, x_2, \ldots, x_n) + g(x_1, x_2, \ldots, x_n)u \\ y &= x_1 \end{aligned} \tag{2}$$

or identically:

$$x^{(n)} = f(x) + g(x)u \tag{3}$$

where, $x^T = [x_1\ x_2\ \ldots\ x_n] = [x\ \dot{x}\ \ldots\ x^{(n-1)}]$ is the system state vector, u is the control input $y = x_1$ is the output f(x) and g(x) are non-linear functions.

The desired bounded state trajectory is defined by $x_r^T = [x_r\ \dot{x}_r\ \ldots\ x_r^{(n-1)}]$ then, the tracking error is defined by $e = x\text{-}x_r = [e\ \dot{e}\ \ldots\ e^{(n-1)}] = [e_1\ e_2\ \ldots\ e_n]$.

$$\dot{e}_n = x^{(n)} - x_r^{(n)} = f(x) + g(x)u - x_r^{(n)} \tag{4}$$

To design the control input u(t) such that X tracks X_r let the sliding surface be defined as:

$$s = \sum_{i=1}^{n-1} k_i e_i + e_n \tag{5}$$

where, $k_i > 0$, i = 1, 2, ..., n-1 are constants which makes the zeros of the polynomial $\lambda^{n-1} + k_{n-1}\lambda^{n-2} + \ldots + k_2\lambda + k_1$ lie in the left side of the imaginary axis in the complex plane and the choice of the coefficients k_i are usually determined by the problem under consideration. Consider the a Lyapunov function as:

$$V = \frac{1}{2g(x)} s^2 \tag{6}$$

If the designed control input u, according to the Lyapunov stability theory makes V negative then the trajectory would be driven and gets attracted to s = 0 and continues to slide till the origin is reached. Differentiation of V along the trajectories gives:

$$\dot{V} = s\,\dot{s} = s\left(\sum_{i=1}^{n-1} k_i e_{i+1} + f(x) + g(x)u - x_r^{(n)} \right) \tag{7}$$

Then, the control input u_1 is chosen as $u_1 = u^*_{eq} + u^*_{eq}$ where u^*_{eq} is the equivalent control term and $u_s{}^*$ the switching control term defined as:

$$u^*_{eq} = \frac{1}{g(x)} \left(-\sum_{i=1}^{n-1} k_i e_{i+1} - f(x) + x_r^{(n)} \right) \tag{8}$$

$$u^*_s(t) = -\frac{k_s}{g(x)} \operatorname{sgn}(s) \tag{9}$$

Where:

$$\operatorname{sgn}(s) = \begin{cases} -1 & s > 0 \\ 0 & s = 0 \\ 1 & s < 0 \end{cases} \tag{10}$$

The control input Eq. 8 with Eq. 9 and 10 guarentees the convergence of the system state trajectory to s = 0 from the initial state.

Single neuron control: An auto tuning single-neuron shown in Fig. 3, reduces the chattering by replacing the SMC when the trajectory goes into the boundary layer. The output of the single neuron given as:

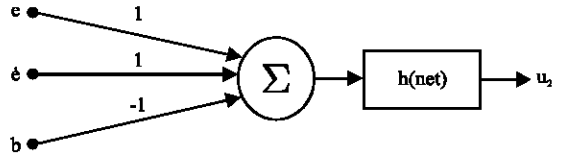

Fig. 3: Structure of a single neuron

$$u_2 = h(net) \tag{11}$$

Where e is the error $e = x-x_r$, b is the bias or threshold, net is weighted sum of inputs $(net = e+\dot{e}-b)$ and the h(net) is the neuron activation function given by:

$$h(net) = \alpha.\frac{1-e^{-(\beta.net)}}{1+e^{-(\beta.net)}} \tag{12}$$

Where α and β are adjustable parameters which affect the output range.

The control output u_2 from Eq.11 can be achieved by online adaptive tuning of the neuron adjustable parameter vector, $\theta = [b, \alpha, \beta]$ which minimizes the Lyapunov function E defined as:

$$E = \frac{(x-x_r)^2}{2} = \frac{e^2}{2} \tag{13}$$

Single neuron-sliding mode control: The control structure of SNSMC combining single neuron with sliding mode controller is shown in Fig. 4.

The output of the combined controller u(t) is a function of individual controller outputs $u_1(t)$ and $u_2(t)$ defined by:

$$u(t) = \begin{cases} u_1(t) & |s(e)| > (\phi+\xi) \\ \delta(e)u_1(t)+(1-\delta(e))u_2(t) & \phi < |s(e)| \le (\phi+\xi) \\ u_2(t) & |s(e)| \le (\phi+\xi) \end{cases} \tag{14}$$

Where s(e) is the switching function defined in Eq. 5, ϕ and ξ are positive boundaries of the layers around the switching function as shown in Fig. 5. $\delta(e)$ is the scaling factor of $u_1(t)$ and $u_2(t)$ which is a function of error defined as:

$$\delta(e) = \frac{|s(e)|-\phi}{\xi} \tag{15}$$

Suspension and torque control of BSRM: The rotor radial position control in x and y directions is achieved by adopting two closed-loop SNSMC controllers independently. The rotor position in both directions is sensed by four displacement sensors and the angular displacement of the rotor is sensed by an encoder.

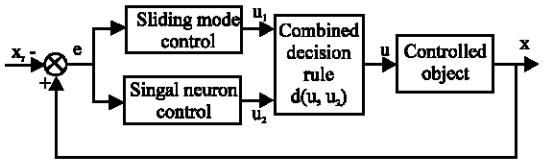

Fig. 4: Combined structure of single neuron and SMC

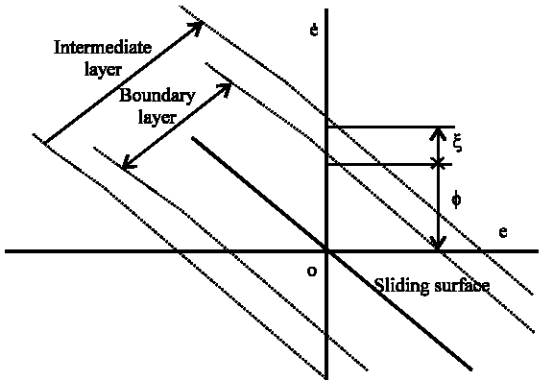

Fig. 5: Boundary and intermediate regions in the phase plane

Table 1: Lookup table

Variables	$+F_x$	$-F_x$
$+F_x$	P_{xp} and P_{yp}	P_{xp} and P_{yn}
$-F_y$	P_{xp} and P_{yn}	P_{xn} and P_{yn}

The suspending force commands F_x^* and F_y^* generated by the two controllers always keep the rotor at the center position using the error between the detected rotor radial displacement and the reference value x^* and y^* in both the directions. For any rotor position, two suspending poles in x and y directions (P_{xp}, P_{xn}, P_{yp} and P_{yn}) and corresponding currents (i_{xp}, i_{xn}, i_{yp} and i_{yn}) are selected using lookup table shown in Table 1.

The current values of selected suspension pole windings are controlled by the current regulated PWM to generate the pulses to the asymmetric converter. The motor speed is regulated by controlling torque using a SNSMC controller, whose input is the error between the reference and the speed detected from the encoder. The output of the controller in the speed loop is the PWM. duty ratio to turning on and turning off of the switches in asymmetric converters of corresponding torque winding phase.

The proposed SNSMC control scheme shown in Fig. 6, illustrates how the 12/14 BSRM's suspension and speed control are achieved simultaneously based on decoupled suspending force and torque.

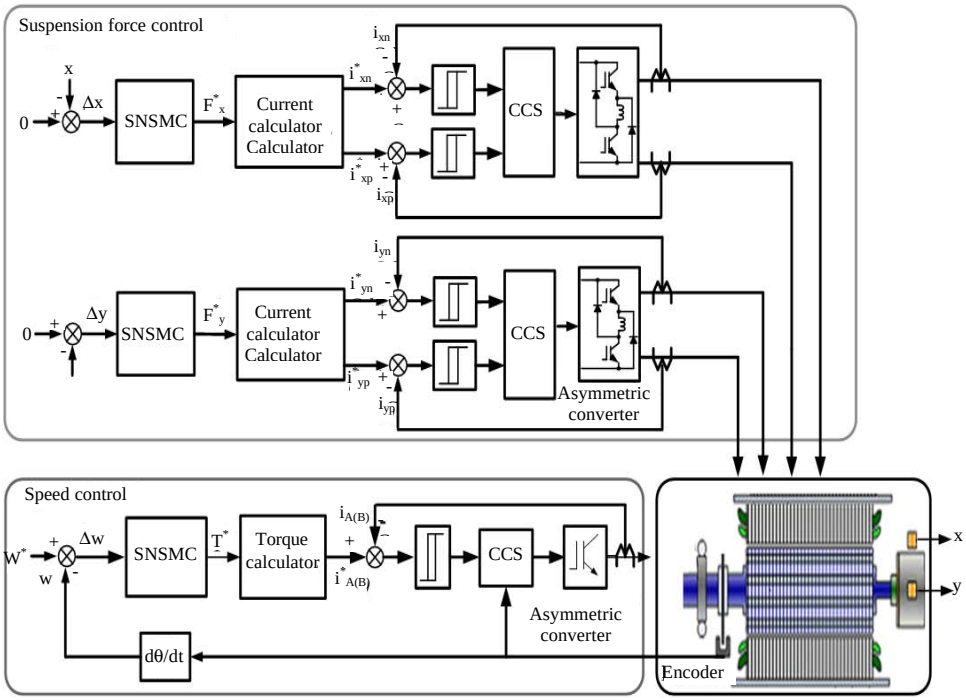

Fig. 6: Block diagram of control scheme

RESULTS AND DISCUSION

To approve the viability and superiority of the proposed control strategy, experiments have been performed on protptype hybrid pole type BSRM and the experimental test setup is shown schematically in Fig. 7. The proposed control scheme is implemented with TMS320F2812 DSP which is compatible with Matlab/Simulink and includes 4 dual PWM channels, 4 ADCs and a speed-encoder input. The encoder generates 2048 pulses per revolution with a supply voltage of 5 V. For independent control asymmetric converters are used for suspending force and torque windings. The BSRM parameters are given in Table 2.

The tuned parameters of SMC are $k_1 = 1.5$, $\phi = 0.08$ and $\xi = 0.1$ and the parameters of the single neuron activation function are taken as $\alpha = 0.3$ and $\beta = 0.1$.

Suspending force control when the rotor is standstil: The experimentation results of rotor displacements in x, y directions and corresponding suspension force currents when the rotor is stationary are shown in Fig. 8. Figure 8 can be seen that the rotor is initially located at 75 μm in the x direction and 80 μm in the y direction and rises quickly to the centre position when SNSMC controller is applied at 200 msec. The corresponsing suspension winding currents are also shown. Since, the torque control is not applied the rotor speed and phase currents are zero.

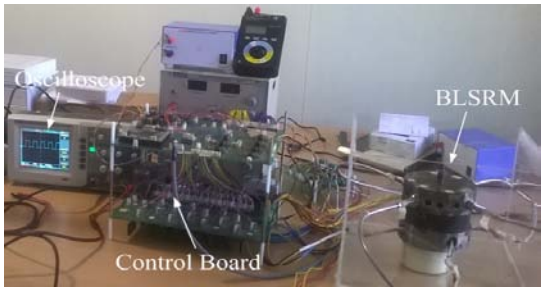

Fig. 7: Experimental setup

Table 2: Parameters of the BSRM

Parameters	Values
No. of poles	
Stator	12
Rotor	14
Pole arc angle	
Torque	12.85°
Suspending force	25.7°
Rotor	12.85°
Length	
Air gap	0.3 mm
Shaft diameter	18 mm
Rotor yoke	9.7 mm
No. of turns in pole windings	
Torque	80
Suspending force	100

Rotor acceleration from rest: Figure 9 shows the results of the suspension and torque control when the rotor speed suddenly changes from rest to 1000 rpm at

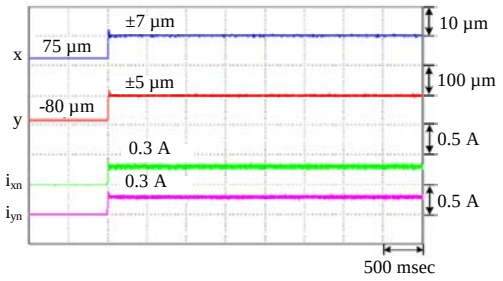

Fig. 8: Rotor displacements and suspension winding currents

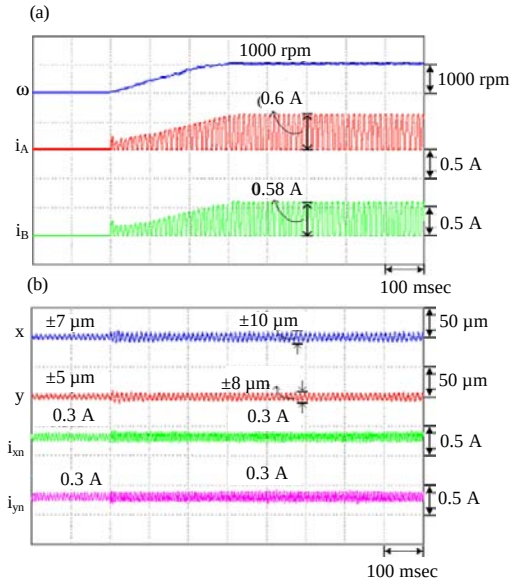

Fig. 9: a) Speed and torque winding currents and b) Rotor displacements, suspension winding currents

200 msec. From Fig. 9a, it is seen that the torque winding currents of phase A and B rises linearly with speed and settle. From Fig. 9b, it can be observed that the rotor suspends steadily with negligible eccentric error, before and after change in speed and the change in corresponding suspending winding currents magnitude remains same.

Variation in speed: Figure 10 shows the results of torque load variation while maintaining the speed at 1000 rpm. As shown in Fig. 10a when torque load is increased from 1-2 N×m at 200 msec, the phase currents increase a little but however, the variation in the motor speed is very little. From Fig. 10b, increase in eccentricity of the rotor is noticed whenever there is a change in load, however the rotor restores back to the center position very quickly. Therefore, it is evident that load variation has almost negligible impact on the suspending force. Figure 11

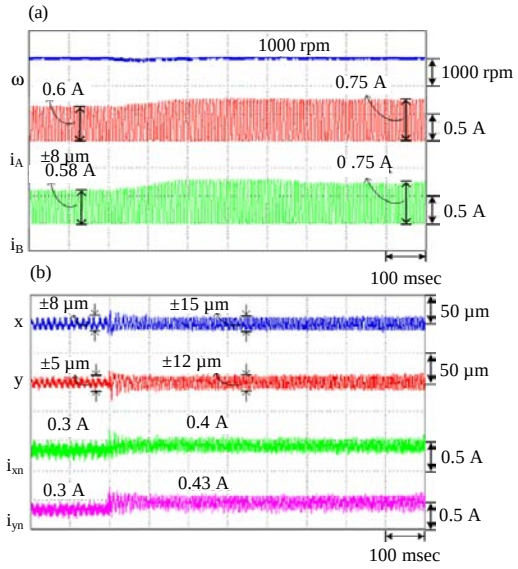

Fig. 10: a) Speed and torque winding current and b) Rotor displacements and suspension winding currents (variation in speed)

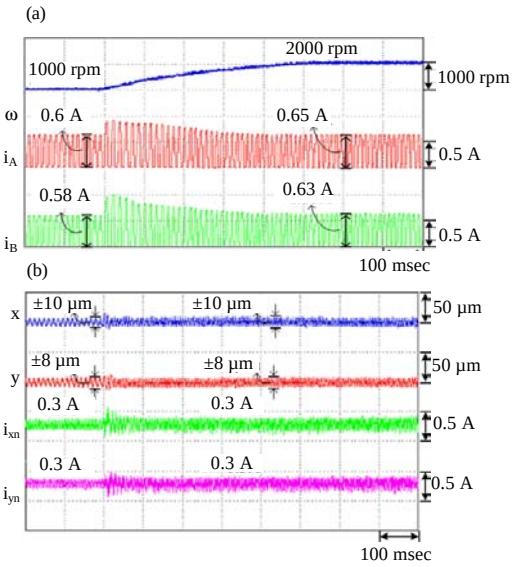

Fig. 11: a) Speed and torque winding current and b) Rotor displacements and load winding currents

shows the results of the torque and suspension control when the rotor speed suddenly changes from 1000-2000 rpm at 200 msec. As shown in Fig. 11a, the torque winding currents of both phases rise suddenly and settle with little increase in value when the speed of the motor is varied. From Fig. 11b, it can be observed that the rotor suspends steadily with negligible eccentric error before and after the change in speed occurs and the change in suspending winding current magnitude remains same.

CONCLUSION

The hybrid pole type BSRM is a multivariable and nonlinear system with unavoidable parameter variations and unmeasured disturbances. The inherent advantage of this motor is a strong decoupling that exists between rotational force and the suspension force which facilitates the independent control of rotor suspension and torque developed. This study proposes a new decoupling control scheme combining the sliding mode control with adaptive single neuron to eliminate chattering without any performance degradation. The experimental results demonstrate that the rotor eccentricity canbe limited to an acceptable range under all possible conditions such as initial suspension, variable speed and load by adjusting the weights of the single neuron in the direction of error minimization.

REFERENCES

Bichsel, J., 1991. The bearingless electrical machine. Proceedings of the International Symposium on Magnetic Suspension Technology, August 19-23, 1991, NASA Publication, Hampton, Virginia, USA., pp: 561-573.

Bosch, R., 1988. Development of a bearingless electric motor. Proceedings of the International Conference on Electric Machines (ICEM'88), September 12-14, 1988, Hemisphere Publishing, Pisa, Italy, pp: 373-375.

Chen, L. and W. Hofmann, 2006. Analytically computing winding currents to generate torque and levitation force of a new bearingless switched reluctance motor. Proceedings of the 12th International Conference on Power Electronics and Motion Control (EPE-PEMC06), August 30-September 1, 2006, IEEE, Portoroz, Slovenia, ISBN:1-4244-0121-6, pp: 1058-1063.

Chen, L. and W. Hofmann, 2007. Performance characteristics of one novel switched reluctance bearingless motor drive. Proceedings of the Conference on Power Conversion (PCC'07), April 2-5, 2007, IEEE, Nagoya, Japan, ISBN:1-4244-0843-1, pp: 608-613.

Fukao, T., 2000. The evolution of motor drive technologies. Proceedings of the 3rd International Conference on Power Electronics and Motion Control (IPEMC 2000) Vol. 1, August 15-18, 2000, IEEE, Beijing, China, ISBN:7-80003-464-X, pp: 33-38.

Hertel, L. and W. Hofmann, 2000. Basic approach for the design of bearingless motors. Proceedings of the 7th International Symposium on Magnetic Bearings, August 23-25, 2000, ETH Zurich, Zurich, Switzerland, pp: 341-346.

Lee, D.H. and J.W. Ahn, 2011. Design and analysis of hybrid stator bearingless SRM. J. Electr. Eng. Technol., 6: 94-103.

Okada, Y., N. Yamashiro, K. Ohmori, T. Masuzawa and T. Yamane *et al*., 2005. Mixed flow artificial heart pump with axial self-bearing motor. IEEE. ASME. Trans. Mechatron., 10: 658-665.

Ooshima, M.S. and C. Takeuchi, 2011. Magnetic suspension performance of a bearingless brushless DC motor for small liquid pumps. IEEE Trans. Ind. Appl., 47: 72-78.

Shen, J.X., K.J. Tseng, D.M. Vilathgamuwa and W.K. Chan, 2000. A novel compact PMSM with magnetic bearing for artificial heart application. IEEE. Trans. Ind. Appl., 36: 1061-1068.

Takemoto, M., A. Chiba and T. Fukao, 2000. A new control method of bearingless switched reluctance motors using square-wave currents. Proceedings of the Conference on Power Engineering Society Winter Meeting Vol. 1, January 23-27, 2000, IEEE, Singapore, ISBN:0-7803-5935-6, pp: 375-380.

Takemoto, M., A. Chiba, H. Akagi and T. Fukao, 2002. Radial force and torque of a bearingless switched reluctance motor operating in a region of magnetic saturation. Proceedings of the 37th IAS Annual Conference on Industry Applications Vol. 1, October 13-18, 2002, IEEE, Pittsburgh, Pennsylvania, USA., ISBN:0-7803-7420-7, pp: 35-42.

Wang, H., D.H. Lee, T.H. Park and J.W. Ahn, 2011. Hybrid stator-pole switched reluctance motor to improve radial force for bearingless application. Energy Convers. Manage., 52: 1371-1376.